EFFECT OF PLASMA TREATMENT ON THE BIOACTIVITY OF POLY(L-LACTIDE) - HYDROXYAPATITE NANO-COMPOSITES

H. Deplaine[1], J.L. Gómez Ribelles[1,2,3], G. Gallego Ferrer[1,2,3]
[1] Centro de Biomateriales e Ingeniería Tisular, Universidad Politécnica de Valencia, P O Box 22012, E-46071 Valencia, Spain
[2] CIBER en Bioingeniería, Biomateriales y Nanomedicina, Valencia, Spain
[3] Centro de Investigación Príncipe Felipe, Valencia, Spain
hardep1@doctor.upv.es

SUMMARY

Poly(L-lactide)/hydroxyapatite composite membranes for bone regeneration with different concentrations of nanoparticles have been prepared and their physicochemical properties and bioactivity have been determined. The treated plasma composites present a faster kinetics of formation of an apatite layer on the surface when immersed into a SBF solution.

Keywords: Poly(L-lactide), hydroxyapatite, nanocomposites, bioactivity, tissue engineering, bone.

INTRODUCTION

Bone regeneration using tissue engineering techniques involve the use of bioresorbable scaffolds that should sustain the load applied *in vivo*. Ceramic materials are brittle and stiff, and macroporous materials made of them are thus fragile, while polymeric materials are unable to sustain the applied loads in many applications [1] Nanocomposites formed by a polymeric matrix reinforced with hydroxyapatite (HAp), other ceramic materials such as tricalciumphosphate, silica or bioactive glass have been proposed in order to design porous materials with adequate mechanical properties for bone engineering [2]. Moreover, the presence of hydroxyapatite nanoparticles can improve the bioactivity of the material, inducing osteogenesis when implanted "in vivo", due to osteoinductive and bone bonding ability [3]. This in vivo behaviour has been shown to be demonstrable by in vitro mineralization (Kokubo test). This experiment was proposed by Kokubo as an "in vitro" test to assess the bioactivity of a material by its capacity to generate a layer of HAp on its surface when immersed in simulated body fluid (thereafter SBF) [4]. The mechanism proposed for this behaviour is that bioactive materials show negative surface potential when immersed in SBF, due to deprotonation at physiological pH of groups like –COOH, -OH, -TiOH (these groups have been shown to provoke hydroxyapatite precipitation in SBF) [5,6]. This negative charge attracts calcium ions, then creating a Ca-rich layer with positive surface potential, which then attracts negative ions in solution like phosphate leading to the deposition of a Ca-poor layer. This process repeats itself generating the HAp layer on the surface of materials [7,8].

For this work poly(L-lactic acid), PLLA was used, since it exhibits mechanical properties suitable for human bone applications. PLLA is a biocompatible and biodegradable polyester belonging to the group of poly α-hydroxy acids, and it can be easily processed into complex shapes. It degrades by non-specific hydrolytic scission of its ester bonds thereby producing lactic acid which is a normal by-product of anaerobic metabolism in the human body [9]. In this work we present a series of PLLA/HAp nano-composites membranes prepared by a freeze extraction process [10]. These membranes were then modified by plasma treatment in order to enhance their bioactivity [11]. As polymer containing carboxylic acids show high plasma susceptibility, the plasma treatment was applied as a help to initiate the nucleation of a layer of HAp. Oxygen plasma permits to lower the surface energy of else hydrophobic PLLA, increasing the wettability and permeability of the membranes to SBF. From previous experiments, it seemed that the particles incorporated in the membranes do not show on the surface since they are covered by a thin layer of PLLA. This thin surface layer is directly attacked by the radicals and electrons of the plasma and thus HAp particles should then show to the surface. Apatite layer formation was observed after different times immersed in SBF as a mean for studying in vitro bioactivity; moreover thermal and mechanical properties of the membranes was studied.

MATERIALS

PURASORB PL 18 PLLA from Purac biomaterials (The Netherlands) was used: it is a homopolymer of L-lactide with an inherent viscosity of 1.8dl/g. 1,4-dioxane was purchased from Scharlau Chemie, S.A.(Barcelona, Spain). Hydroxyapatite particles with particle size inferior to 200nm were purchased from SIGMA-ALDRICH (Spain). The chemicals used in the preparation of SBF were from SIGMA-ALDRICH(Spain). All chemicals were used as received without any further purification.

METHODS

Sample preparation

A series of poly-L-lactic acid/hydroxyapatite composite membranes with HAp content 0, 5, 15, and 20% (w/w) were prepared by freeze extraction method. Freeze extraction is a modification of freeze drying process described by Ho et al [**Error! Bookmark not defined.**]. Shortly, the required quantity of HAp powder was dispersed in dioxane by sonication, then a 15% weight PLLA was added to the mixtures, and stirred to complete dissolution. Four solutions with different content in HAp were prepared, with 0, 5, 10, 15% particles by weight with regard to PLLA. The PLLA-HAp solutions were poured into Teflon moulds and frozen in liquid nitrogen. Then, cold ethanol at -10ºC was poured on the frozen membranes in order to dissolve the crystallized dioxane. Dioxane extraction was conducted in a cold ethanol bath at -10ºC, ethanol was changed until the dioxane had completely disappeared from the structure. After extraction, membranes were dried in air atmosphere during 24h and then in vacuum to constant weight at room temperature. The membranes were cut into squares (1cm x 1cm) of 200μm thickness. These samples were shaped included in OCT at -30ºC and cut by cryogenic microtome. After removing residues of OCT, samples were dried first at room temperature for 24

hours and then under vacuum 24 hours and then under vacuum at 40ºC for 24 hours more.

Bioactivity test

SBF solution was prepared with the method of Müller et al. [12] from five mother solutions of, KCl (59.64 g/l), NaCl(116.88 g/l), $NaHCO_3$(45.37g/l), $MgSO_4.7H_2O$(49.30 g/l), $CaCl_2$(14.702g/l), TRIS (tris-hydroxymethyl aminomethan; 121.16 g/l) (used for pH adjustment, see below), NaN_3(1 g/l), KH_2PO_4(27.22 g/l) into 650 ml deionised ultra pure water, in order to prevent salt precipitation and maintain the pH of the solution. Then the solution was poured in a 1000ml flask and filled up with deionised ultra pure water. For pH adjustment TRIS-base buffer was prepared by dissolving TRIS-base in deionised ultra pure water, and adjusting pH of the solution by adding HCl till pH 7.6-7.7 at 25ºC (which corresponds to pH 7.3-7.4 at 37ºC).

Table 1. Concentrated solutions volumes used for 1L of SBF

Salts	KCl	NaCl	$NaHCO_3$	$MgSO_4.7H_2O$	CaCl	Tris.HCl	NaN_3	KH_2PO_4
volume (ml)	5	60	10	5	25	50	10	5

Oxygen plasma treatment

Surface modification was carried out with oxygen plasma (Plasma Electronic, model Piccolo, quartz cylinder, 2.45 GHz generator) under 300W under 50 Pa vacuum, during 120 seconds for each side. Membranes were used for experiments immediately after exposure.

Differential scanning calorimetry (DSC)

Crystallinity was evaluated by thermal analysis with a PERKIN ELMER DSC Pyris I. Two heating scans from 0ºC to 210ºC at 10ºC/min were performed, the first one in order to gain information on sample crystalinity after freeze extraction process, and the second one in order to observe the behaviour of the samples after erasing thermal history and cooling down from 210ºC to 0ºC at 10ºC/min.

Calcination experiments

The real content of HA in the composites was determined by weighing membrane residues after calcination. Calcination was carried out in a Conatec HC-300 ceramic oven. For each concentration (0-5-10-15% wt. HAp), three samples were heated up to 600ºC at 10ºC/min, and maintained at 600ºC during 10 minutes, in order to entirely thermally degrade the PLLA.

Dynamic mechanical thermal analysis (DMTA)

The dynamic mechanical analysis of the membranes before immersing in SBF were determined the Seiko Instruments EXTRAR6000 Thermal Analysis and Rheology System. The samples were heated first from 0ºC up to 120ºC at 2ºC/min, maintained at 120ºC during 60 minutes, and then cooled down to 0ºC at 2ºC and heated again up to

150ºC. Testing frequency was 1 Hz, the membranes presented rectangular dimensions 3 x3 x30 mm.

HAp morphology analysis and characterization

For scanning electron microscope analysis, samples were mounted onto copper holders and gold sputtered. The morphology of the HAp formed on the surface of the scaffold was characterized with a JEOL JSM 6300 scanning electron in secondary mode under an acceleration tension of 15kV.

HAp layer characterization

For EDS analysis, samples were mounted onto copper holders and carbon sputtered. Elements quantification was preformed by Electron Dispersive Spectrosmetry, EDS, with a JEOL JSM 6300 scanning electron microscope with an acceleration tension of 10kV. The samples were observed by SEM and EDX after 0, 7, 14 and 21 days in SBF with and without oxygen plasma treatment.

RESULTS AND DISCUSSION

Membranes characterization

The freeze extraction process produces a membrane with 10 μm micropores as shown in Figure 1. The micropores are homogenously dispersed on the surface of the membranes [10]. To assure the reproducibility of the technique, 3 different membranes were fabricated and observed by SEM. All membranes exhibited the same morphology. The pores are produced by the phase separation when both dioxane and PLLA crystallizes from the solution. When producing a nanocomposite membrane, the HAp nanoparticles are suspended in the solution. Crystallization of PLLA entraps part of these particles but another part is expected to rest between dioxane crystals or at the interfaces between dioxane and PLLA in the solid sample when immersed in liquid nitrogen.

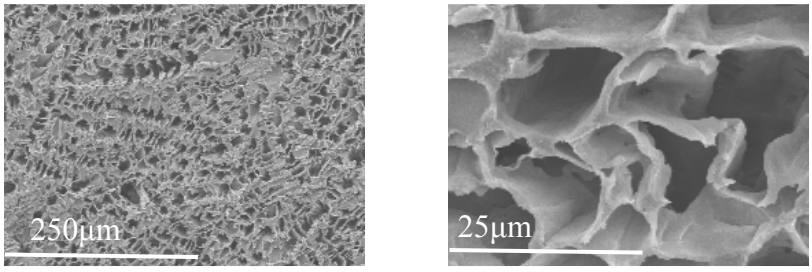

Figure 1. SEM microphotographs of the surface of PLLA membranes before immersing in SBF

The morphology of the membranes seems not to be affected by plasma treatment. After oxygen plasma treatment, as shown on figure 2 some kind of abrasion defects can be seen on the surface of the membranes, which does not appear for the membranes without plasma treatment. Surface abrasion that was already found in plasma treated PLLA by Wang et al [11] can allow HAp particles to appear at the pores walls.

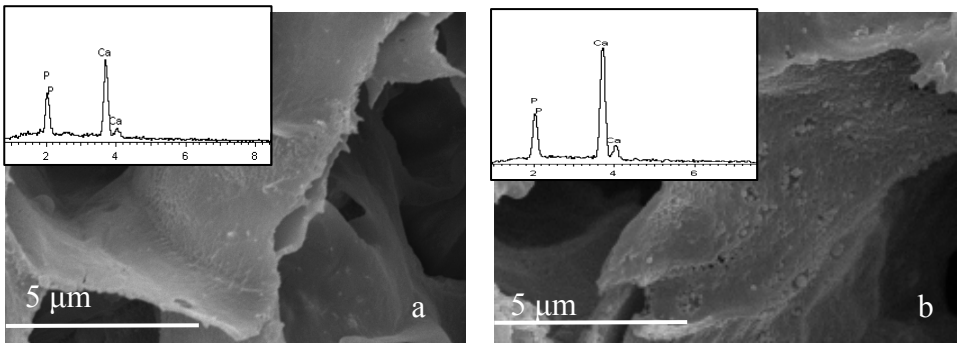

Figure 2. SEM and EDS analysis of PLLA/HAp nanocomposites with 10% wt. of HAp, 0 days in SBF a) without plasma treatment, b) with plasma treatment.

Although HAp nanoparticles cannot be seen by SEM, especially in the untreated membranes, probably because a layer of PLLA covers them, EDS analysis was able to show Ca and P peaks distinctive of the HAp components as shown by the inserts of figures 2a and 2b. The EDS analysis was repeated three times in different zones for three different samples, and all the signals present the same behaviour, proving that particle dispersion is homogenous.

Calcination experiments

Table 2. Mass difference after and before calcination

HAp content (%)	HAp incorporated mass measured	HAp incorporated theoretical mass	HAp content error (%)
0	0.002 ±0.006	0.000	0
5	0.042 ±0.004	0.048 ±0.005	12
10	0.074 ±0.006	0.084 ±0.007	12
15	0.073 ±0.010	0.092 ±0.008	21

The calcination experiments showed that the amount of HAp incorporated into the membranes is close but lower than the amount of HAp dispersed in the PLLA solution. Membranes with 5, 10% HAp (table 2) show 12% mass error, and 15% HAp membrane mass error is of 21%. Possible reasons for this deviation are to seek in the imperfect dispersion of particles, or the leaching of a part of the particles that remained in the solvent phase during phase separation.

Differential scanning calorimetry (DSC)

DSC experiments included a first heating scan that gives information about the crystalline structure obtained after freeze extraction process. This scan was performed between 0 and 210ºC. Thus, at the end of this scan the sample is melted. A cooling scan followed to characterize the crystallization kinetics from the melt of the different nanocomposites. Finally a second heating scan was recorded to characterize the structure of the polymer crystallized from the melt.

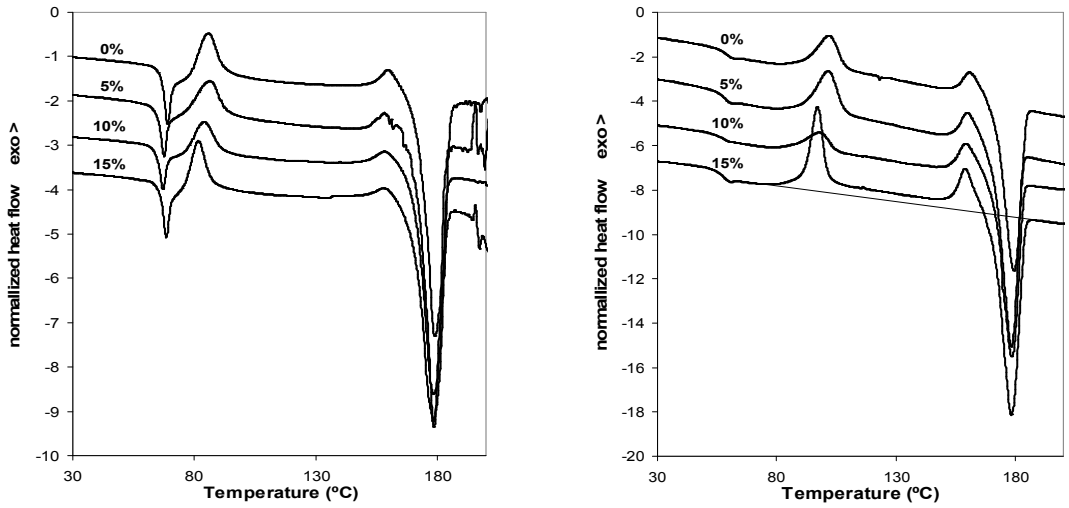

Figure 3 First DSC heating scan of PLLA/HAp nanocomposite with different filler content (left), and second DSC heating scan (right).

First heating scan shows the glass transition with a large overshoot characteristic of the physical ageing (or structural relaxation) process suffered by the polymer during annealing at 40ºC while drying in vacuum. At higher temperatures cold crystallization exothermal appears at lower temperatures as the HAp nanoparticles content increases (see Figure 3, left). Another crystallization process appears at higher temperatures that is characteristic of highly nucleated samples that crystallize at very low temperatures [13], finally the melting process takes place at a temperature independent of sample composition. Cooling scan recorded after the first heating scan showed an exothermal peak (results not shown) that proves that PLLA partially crystallizes on cooling.

Second scan is representative of the samples crystallized from the melt, here the endothermal overshoot due to physical ageing disappears since the sample was not annealed below the glass transition (Figure 3, right). The crystallization and melting follow a trend similar to that of the first scan although the first exothermal is clearly shifted towards higher temperatures. This behaviour can be explained by the formation of crystalline nuclei during physical ageing at temperatures below T_g that has been proven in PLLA [13] and in other semicrystalline polymers as well [13]. An increased number of nuclei at the beginning of cold crystallization speeds up the process; as a result the observed crystallization peak is sharper and shifted towards lower temperatures. The changes in shape and position for cold crystallization peaks with increasing HAp content demonstrates in the same manner the nucleating effect of the HAp nanoparticles.

The baseline used for the determination of crystallinity in the sample is represented as an example in Figure 4 in the thermogram corresponding to the second scan of the 15% HAp composite. The determination of crystallinity was done by an integration of the heat flow trace with respect to it. This linear baseline joints a point immediately above the glass transition and another one after melting. If the sample were completely amorphous at the beginning of the heating scan the area between the thermogram and the baseline would be zero. The calculus becomes quite uncertain since the temperature

interval to which it is extended is very broad and lead easily to small errors in the determination of the baseline used in the integration (for instance for small curvatures in the baseline of the calorimeter). This difficulty is especially clear in the first scan when the thermogram starts deviating towards the exothermal side immediately above the glass transition (Figure 3, left), which impedes any enthalpy calculation. In the second scan crystallinity values between 6 and 20% were found but the HAp content dependence was non-systematic. The onset of the glass transition seems to be independent on the filler content, the difference between the values measured in the first and second scan should be due to the physical ageing process to which samples were subjected during drying before the first scan. A slight decrease of the enthalpic glass transition temperature with the HAp content is observed(Table 3).

Table 3. Glass transition temperatures DSC and values of storage modulus during second DMTA heating scan as a function of the HAp content of the membranes

HAp content (%)	Tg onset first heating	Tg onset second heating	enthalpic Tg	E' glass first scan (30ºC)	E' glass second scan (30ºC)	E' rubber second scan (120ºC)
0%	51	36	62	1.81E+08	2.03E+08	1.20E+07
5%	48	38	58	2.02E+08	2.30E+08	1.43E+07
10%	51	38	58	2.37E+08	2.68E+08	1.60E+07
15%	49	37	55	2.56E+08	3.03E+08	1.69E+07

Dynamic mechanical thermal analysis (DMTA)

Dynamic-mechanical experiments are also highly dependent on the thermal treatment to which the sample is subjected. The samples were first subjected to heating from 0 and 120ºC in the first measuring scan. The temperature dependence of the storage modulus, E' shows the sharp decrease starting close to the calorimetric glass transition. The shape of the curve with a change of slope in the middle of the relaxation yields to think that crystallization starts during the scan itself, as seen in the DMTA curves (Figure 4a), this makes the values measured at temperatures above T_g quite dependent on the thermal history in the scan itself. The modulus in the glass region measured in the first scan increases with the HAp content of the composites (Table 1) what shows the reinforcing role of the HAp particles. To compare the behaviour of the different nanocomposites with a more reproducible structure, samples were annealed at 120ºC for one hour to allow crystallization and cooled to 0ºC to start the second scan. Thus, the second scan corresponds to higher crystallinity samples. The main relaxation in the second scan is shifted to higher temperatures with respect to the first one, the value of E' in the glassy region increases with respect to the first scan due to the higher fraction of PLLA crystals and the reinforcing effect of the nanoparticles is clearly shown in the semicrystalline samples both below and above the glass transition of the amorphous phase (Figure 4b).

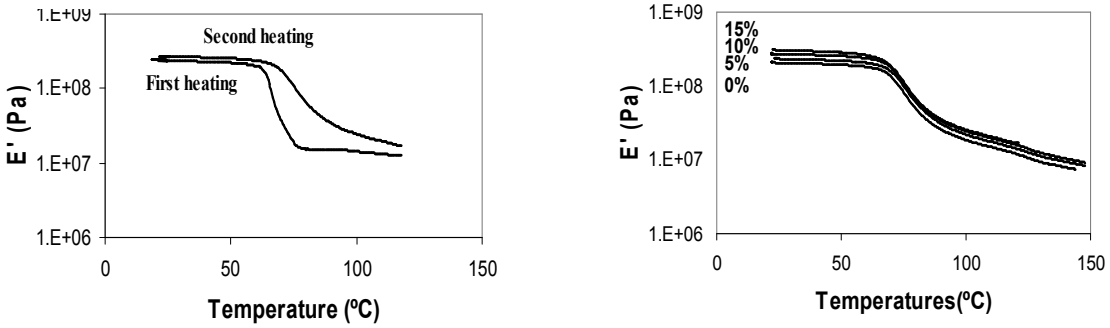

Figure 4 .a)E'(T) representation in first and second heating scan of 10% HAp membranes b) E'(T) representation from second heating scan of 0, 5, 10, 15% HAp membranes during DMTA experiment

SEM analysis shows the influence on the kinetics of HAp deposition during increasing immersion times in SBF. As noticed in figure 5 PLLA is able to nucleate HAp in is surface, without any special treatment but at very slow rates compared to plasma-treated PLLA or PLLA reinforced with HAp. At short times a few nuclei can be observed in the SEM pictures that increase in number to form a rough layer of cauliflower-shaped crystals [14]. The surface of the micropores appears uniformly coated by HAp after an immersion time that decreases as the content of HAp in the composite increases and with the plasma treatment. In order to show this behaviour with a reasonable number of figures, Figure 5 shows the surface of a PLLA membrane after 21 days of immersion in SBF, a time at which coating is still not complete, whereas the sample treated with plasma show a smooth layer of biomimetic HAp deposited on the surface.

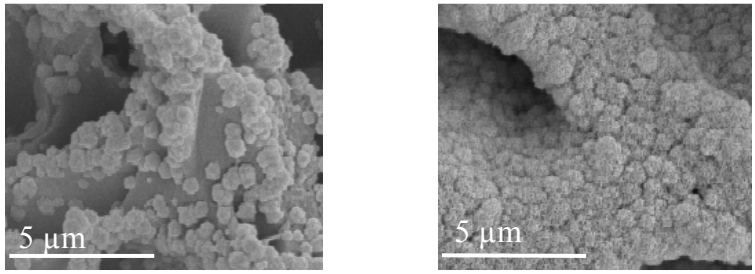

Figure 5. SEM analysis of pure PLLA membranes, without plasma treatment (left) and with oxygen plasma treatment (right), after 21 days in SBF

Figure 6 shows the effect of the HAp nanofiller content after 7 days immersion. The PLLA samples shows after this time no signs of apatite layer even when treated with plasma, but the rate of deposition increases with HAp content and samples containing more than 10% HAp nanoparticles shows a smooth coating of the composite surfaces. Plasma treatment further enhance the rate of deposition and the thickness of the layer increases in such a way that biomimetic apatite fills the whole volume of the micropores (Figure 6). Results obtained after different immersion times in SBF (7, 14, 21 days) are similar. Figure 6 shows the typical cauliflowers structure of the HAp of the layer on the surface.

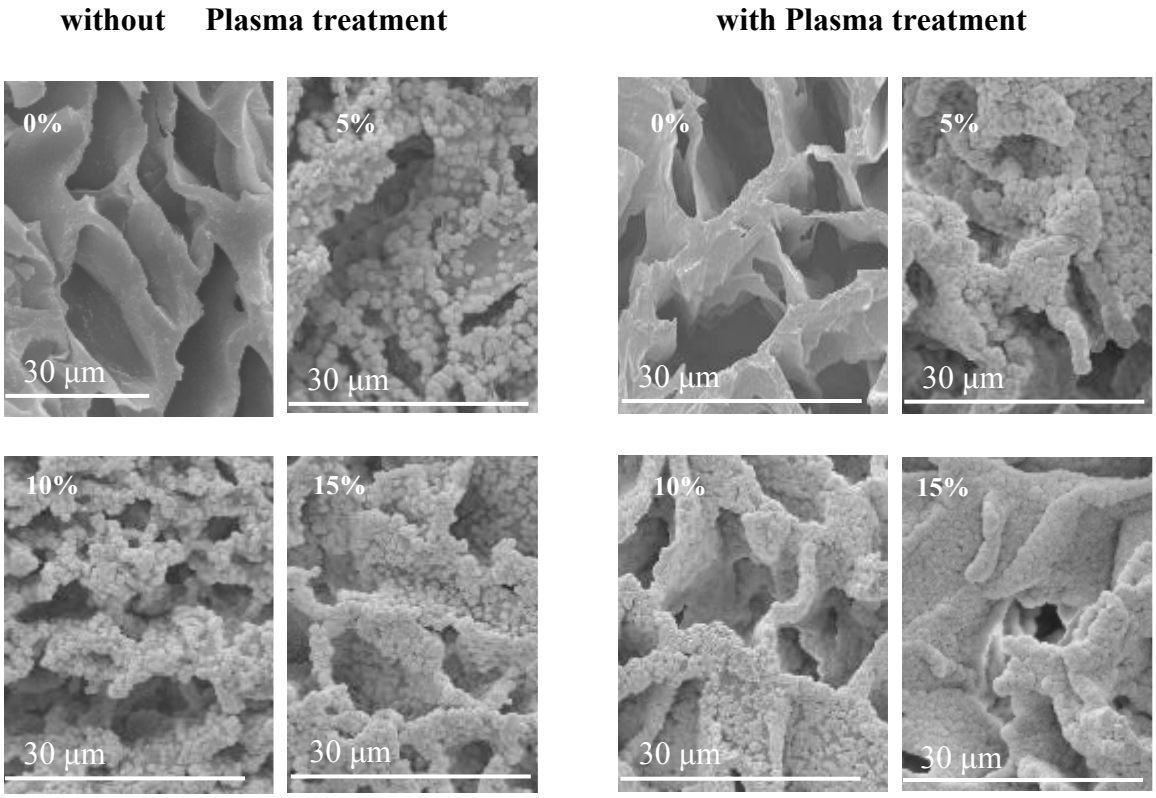

Figure 6. SEM analysis of 0, 5, 10, 15% HAp membranes without and with out oxygen plasma treatment, after 7 days in SBF

Table 5. Ca/P atomic ratio reported from EDS analysis

Immersion time (days)	0		7		14		21	
HAp content (%)	untreated	plasma treated	untreated	plasma treated	untreated	plasma treated	untreated	plasma treated
0	0 ±0	0±0	0±0	0±0	-	-	2.18 ±0.6	1.77 ±0.4
5	2.54 ±0.5	2.15 ±0.4	1.82 ±0.1	**1.66 ±0.1**	-	-	2.55 ±0.7	1.77 ±0.3
10	2.1 ±0.2	2.38 ±0.4	1.68 ±0.05	**1.67 ±0.05**	2.25 ±0.7	1.95 ±0.2	2.2 ±0.3	2.48 ±1.3
15	2.21 ±0.3	2.33 ±0.4	1.63 ±0.1	**1.69 ±0.2**	-	-	2.08 ±0.2	2.62 ±1.4

As can be seen on table 5, Ca/P atomic ratio has been calculated from EDS measurements in each case to be compared with that of stoichiometric hydroxyapatite ($Ca_{10}(PO_4)_6(OH)_2$) Ca/P = 1.67, or physiological HAp = 1.65. Globally the Ca/P atomic ratio calculated for all the samples is higher than the physiological HAp one, oscillating between 1.63 to 2.54 (table 5) [15]. The membranes with HAp incorporated at day 0, in which the Ca/P atomic ratio measured corresponds to the HAp nanoparticles added as filler, have the highest ratio, and the ratio observed doesn't match that of stoichiometric hydroxyapatite claimed by the supplier. For the same immersion time membranes previously exposed to plasma present a ratio closer to the physiological one in comparison with membranes that had not been exposed to plasma. Globally, the ratio that is closest to the physiological one is for the plasma treated membranes after 7 days in SBF.

CONCLUSIONS

Freeze extraction allows obtaining PLLA / HAp nanocomposites with a good dispersion of HAp particles and bioactive properties. The elastic modulus increases with the filler content at temperatures above and below the glass transition of the amorphous phase. Particles act as a nucleating agent for PLLA modifying the crystallization kinetics whereas glass transition temperature of PLLA is independent of the filler content. The bioactivity is enhanced by the presence of the HAp particles more than by plasma treatment; indeed the nucleation of a biomimetic HAp layer on the surface of the nanocomposites when immersed in SBF is more effective than on PLLA membranes. These materials may be used in the future as scaffolds for bone tissue engineering.

ACKNOWLEDGEMENTS

The authors acknowledge the support of the Spanish Ministery of Science and Innovation trough the DPI2007-65601-C03-03 project. Dr. G. Gallego Ferrer acknowledges the support of the same Institution for the mobility grant JC2008-00135 in the "José Castillejo" program to do a research stay in the 3Bs Group of the Polymers Department of the University of Minho, Portugal.

References

1 Karlis A. Gross, Luis M. Rodriguez-Lorenzo. Biomaterials 25 (2004) 4955–4962.
2 Molly M.Stevens. Materials today may 2008 volume 11 number 5.
3 Murphy WL, Hsiong S, Richardson TP, Simmons CA, Mooney DJ. Biomaterials 26 (2006) 303-310.
4 Tadashi Kokubo, Hiroai Takadama. Biomaterials 27 (2006) 2907-2915.
5 Oliveira AL, Mano JF, Reis RL. Current Opinion in Solid State and Materials Science 2003;7(4-5):309-318.
6 Kawashita M, Nakao M, Minoda M, Kim HM, Beppu T, Miyamoto T, et al. Biomaterials 2003;24(14):2477-2484.
7 Landi E, Tampieri A, Celotti G, Langenati R, Sandri M, Sprio S. Biomaterials 2005;26(16):2835-2845.
8 Hyun-Min Kim, Teruyuki Himeno, Tadashi Kokubo, Takashi Nakamura. Biomaterials 26 (2005) 4366–4373
9 Guobao Wei, Peter X.Ma. "Polymer/Ceramic composite scaffolds for bone tissue engineering. In "Scaffolding in tissue engineering" Peter X. Ma, Jennifer Elisseeff. Taylor and Francis Group chapter 9 page 241.
10 M. Lebourg, J. Suay Antón, J.L. Gómez Ribelles. European Polymer Journal 44 (2008) 2207–2218.
11 Xue Qu, Wenjin Cui, Fei Yang, Changchun Min, Hong Shen, Jianzhong Bei, Shenguo Wang. Biomaterials 28 (2007) 9–18.
12 Lenka Müller, Frank A. Müller. Acta Biomaterialia 2 (2006) 181–189.
13 F. Hernández, J. Molina Mateo, F. Romero Colomer, M. Salmerón Sánchez, J.L. Gómez Ribelles, J. Mano .Biomacromolecules 6(6), 3291-3299 (2005)
14 Zhongkui Hong, Rui L.Reis, João F.Mano. Acta Biomaterialia 4 (2008) 1297–1306.
15 Vallés Lluch A, Gallego Ferrer G, Monleón Pradas M, Polymer (2009), in press, doi:10.1016/j.polymer.2009.04.022.